Cyclic tests on bolted steel and composite double-sided beam-to-column joints

Dan Dubina†, Adrian Liviu Ciutina‡ and Aurel Stratan‡

Department of Steel Structures and Structural Mechanics, Faculty of Civil Engineering and Architecture, "Politehnica" University of Timisoara, I. Curea nr.1, Timisoara 1900, Romania

Abstract. This paper summarises results of the research performed at the Department of Steel Structures and Structural Mechanics from the "Politehnica" University of Timisoara, Romania, in order to evaluate the performance of beam-to-column extended end plate connections for steel and composite joints. It comprises laboratory tests on steel and composite joints, and numerical modelling of joints, based on tests. Tested joints are double-sided, with structural elements realised of welded steel sections. The columns are of cruciform cross-section, while the beams are of I section. Both monotonic and cyclic loading, symmetrically and anti-symmetrically, has been applied. On the basis of tested joints, a refined computer model has been calibrated using a special connection element of the computer code DRAIN 2DX. In this way, a static/dynamic structural analysis of framed structures with real characteristics of the beam to column joints is possible.

Keywords: beam-to column joints; steel joints; composite joints; experimental tests; ductility; resistance; joint modelling; structural analysis.

1. Introduction

The key points in the behaviour of Moment Resisting Steel Frames (MRSF) are the beam-to-column joints, located near the dissipative zones. These should posses adequate rotation capacity and resistance in order to resist the earthquake action.

Laboratory tests performed in Timisoara on double-sided beam-to-column joints made up of European standard I-shaped profiles (Dubina *et al*. 2000a, Dubina *et al*. 2001) have shown important differences in the behaviour of joints subjected to gravitational loads (balanced moments), and horizontal seismic loads (unbalanced moments). Anti-symmetrical loading has led to a smaller moment capacity and stiffness, and a substantial increase in the rotational ductility of the joint, as compared to symmetrically loaded joints. The difference of joint behaviour was given by the column web panel, which is not subjected to shear in case of symmetrically loaded joints.

An alternative to the "standard" European column cross-section (hot-rolled I profiles) is the use of X-shaped cross-sections, built-up of two hot-rolled profiles welded along the median axis or built-up sections made out from welded plates, as shown in Fig. 1.

Generally, this type of cross-section is used for space moment resisting frames, due to its similar stiffness in both directions and its convenience for three- and four-way moment connections. Joints to
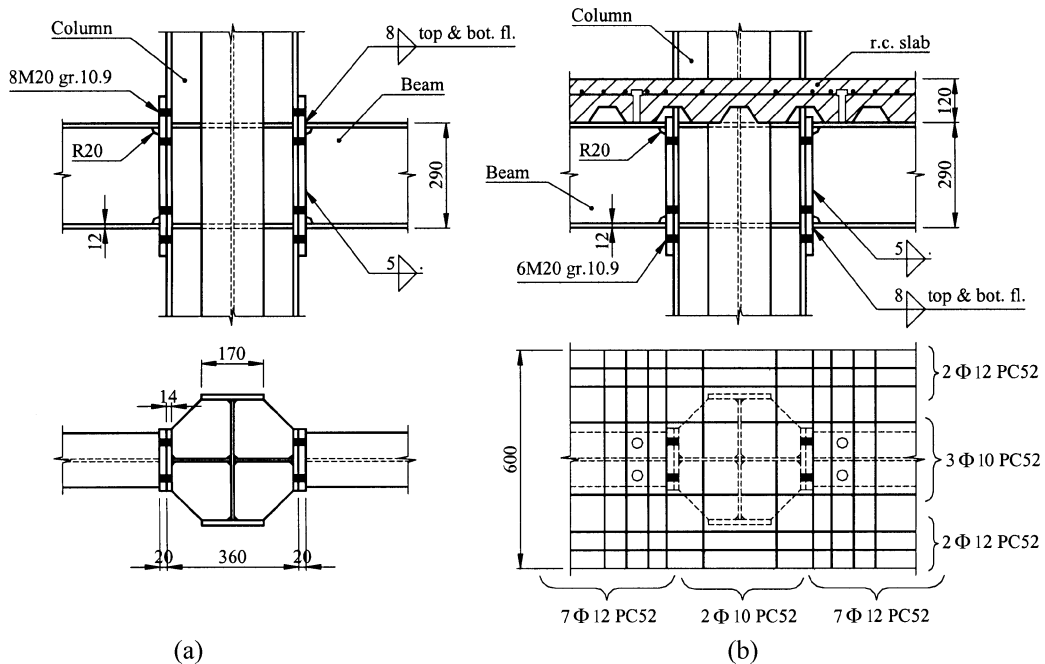
---

†Professor
‡Ph.D Student

Fig. 1 Connection configurations for BX-S series (a) and BX-C series (b) of joints

X-shaped columns have not been tested particularly in the past. The experimental program carried out at the Laboratory of Steel Structures from the "Politehnica" University of Timisoara comprised both bare-steel (BX-S series) and composite joints (BX-C series) with extended end-plates, I-shaped beams and X-shaped columns (Fig. 1) tested under symmetrical and anti-symmetrical loading.

In order to evaluate the performance of a structure by global analysis, accurate modelling for both members (beams and columns) and connections are needed. The usual models for connections are either pinned or fully-rigid models, or models based on bilinear characteristic M-F curves. A more accurate M-F model in case of connections could give results closer to the real structural behaviour (Ciutina *et al*. 2001). Based on the above-described experiments, a calibration of the experimental curves was undertaken using the DRAIN 2DX computer code, using a multi-linear *M-Φ* curve (element 14).

2. Experimental tests on bare-steel joints

The testing program comprised six specimens: three joints under symmetrical loading (BX-SS, see Fig. 2a), and three joints under anti-symmetrical loading (BX-SU, see Fig. 2b). The bolts have been fully preloaded, except for the last joint of each series, which have been preloaded to 50% only. Tests were performed in accordance with the ECCS Recommendations complete procedure (ECCS 1985 see Fig. 3). The first specimen from each series was tested monotonically, in order to determine the conventional yield displacement e_y. Specimen failure was considered at 50% reduction of the maximum load applied during the loading history. The load was applied quasi-statically, under displacement control.

Steel characteristics of the main joint components according to mill certificates and conducted tensile tests are presented in Table 1. Results of the coupon tests show that the steel is S275 grade ($f_y = 270$ N/mm²,
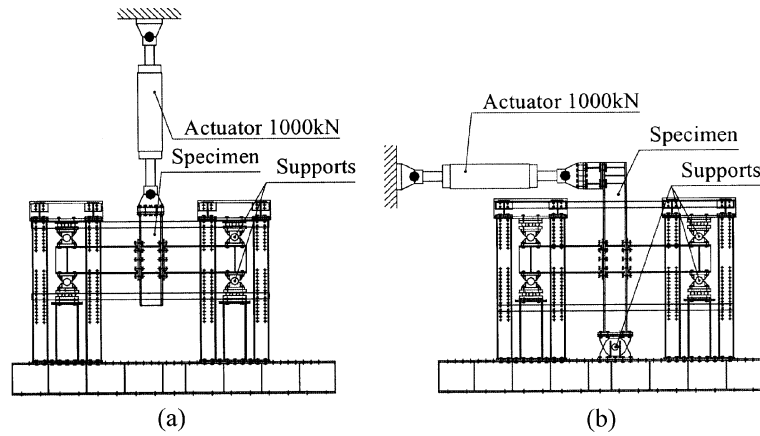
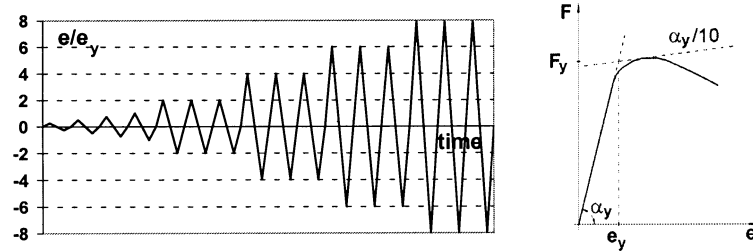Fig. 2 Testing set-up for symmetrical loading (a) and for anti-symmetrical loading (b)

Fig. 3 ECCS loading procedure and determination of test characteristics

$f_u = 430$ N/mm^2) instead of the specified S235, also confirmed by studies on the chemical composition of the end plate material (Moisa 2000).

Table 2 and Figs. 4a, 5, and 6 synthetically present the behaviour of tested specimens, while Table 3 shows the main experimental results expressed in terms of maximum plastic rotation φ_{max}, maximum moment attained M_{max}, and the cumulated energy dissipated by the specimens during the entire loading history E_{tot}.

3. Experimental tests on composite joints

Table 1 Characteristics of main steel components

Design grade	Element		Yield stress, f_y [N/mm^2]		Tensile strength, f_u [N/mm^2]	
			Mill	Coupon	Mill	Coupon
S235 f_y–240 f_u–360	Beam	flange	303.0	303.0	391.0	470.6
		web	258.0	316.2	400.0	455.7
	Column	flange	258.0	295.2	400.0	444.2
		web	258.0	316.2	400.0	455.7
	End plate		235.0	368.5	421.0	550.2

Table 2 Behaviour of bare-steel joints

Specimen	Observed behaviour
BX-SS-M (monotonic loading)	$3e_y$ - visible deformations of the end plate in the tension zone; $6\text{-}8e_y$ - significant bending of column flanges; $9.5e_y$ (0.03 rad) bolt failure (see Fig. 4a); $12e_y$ (0.043 rad) general
BX-SS-C1 (cyclic loading)	$4\text{-}6e_y$ - plastic deformations of end plate and column flanges; 1st $8e_y$ - brittle failure of the lower beam flange to end plate weld; cracking of the beam web to end plate weld, and failure of the superior flange weld during load reversal
BX-SS-C2 (cyclic loading)	$4\text{-}6e_y$ - plastic deformations of end plate and column flanges; 3rd $6e_y$ - brittle failure of the lower beam flange to end plate weld (see Fig. 6a); failure of the superior flange weld during load reversal
BX-SU-M (monotonic loading)	$1\text{-}2e_y$ - shearing of the panel zone; $4e_y$ - bending of the end plate and column flanges; $5e_y$ - beam flange buckling; $10.5e_y$ (0.096 rad) - failure of a bolt from the extended part of the end plate (see Fig. 4a); $11.5e_y$ (0.11 rad) - failure of the second bolt from the same row
BX-SU-C1 (cyclic loading)	$4e_y$ - plastic deformations of the end plate, column flanges, and shearing of the panel zone; 1st and 2nd $6e_y$ - cracking of beam flange to end plate welds, propagated into the end plate (cracking of the end plate followed two patterns: lamellar tearing at the superior part and through-thickness cracking at the inferior part see Fig. 6b); 3rd $6e_y$ - bolt failure in the extended part of the end plate
BX-SU-C2 (cyclic loading)	3rd $4e_y$ and 1st $6e_y$ - cracks in the beam flange to end plate welds, leading to lamellar tearing of the end plate; 2nd $6e_y$ - failure of 5 bolts from the left connection

(a)   (b)

Fig. 4 Failure of the BX-SS-M (a) and BX-CS-M1 (b) specimens

The steel part of the composite joints is similar to the bare-steel joints, except the end-plate, which is extended only at the bottom part (see Fig. 1), following the rationale that the slab reinforcement will compensate the missing bolt row at the top. The r.c. slab has a total depth of 120 mm, lying on a LINDAB LTP45×0.7 corrugated sheet. The slab width was taken equal to the effective width of the
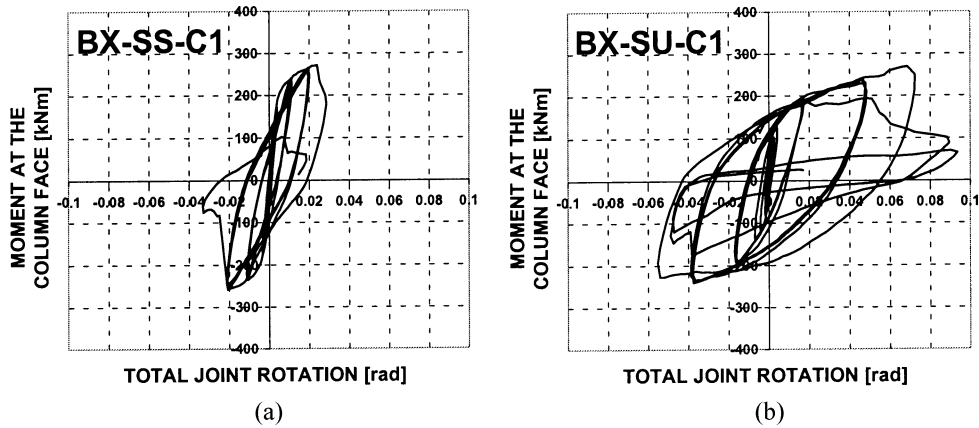
Fig. 5 Moment - rotation relationships for cyclic specimens of the BX-S series
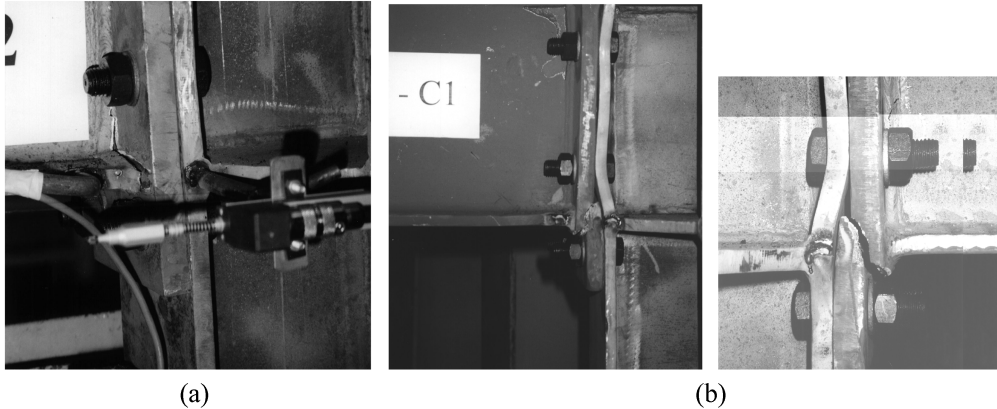

Fig. 6 BX-SS-C2: Weld failure (a); BX-SU-C1: End plate failure (b)

slab, computed according to Eurocode 4 (1992). Member dimensions and effective slab width have been determined by designing a three-bay (3×4.5 m), three-storey (3×3.5 m) moment resisting frame. The effective width of the slab is relatively small (600 mm), this needs to be recognised when considering the conclusions of the present study. Nelson connectors have been used, to achieve a full shear connection between the beam and the slab.

The experimental program comprised three symmetrically loaded specimens (BX-CS series: one tested monotonically to negative moments - BX-CS-M1, one tested monotonically to positive moments - BX-CS-M2, and the third one tested under cyclic loading - BX-CS-C1) and three anti-symmetrical loading (BX-CU series: one tested monotonically - BX-CU-M, and the other two cyclically - BX-CU-C1 and BX-CU-C2). In the case of the BX-CU-C2 specimen, the ECCS procedure was not applied, instead, constant cycles of $6e_y$ were used. In the case of composite joints all the bolts have been preloaded to 100% of the full preloading value.

The specified concrete for the slab was C20/25. However, compression tests performed on 141 mm cube specimens showed a mean resistance of 18.5 N/mm². The characteristics of the steel reinforcement is:

Dan Dubina, Adrian Liviu Ciutina and Aurel Stratan

Table 3 Experimental results for bare-steel joints

Specimen	φ_{max}^+, rad	φ_{max}^-, rad	M_{max}^+, kNm	M_{max}^-, kNm	E_{tot}, kNm rad
BX-SS-M	0.043	-	263.3	-	9.0
BX-SS-C1	0.028	0.021	271.6	259.1	41.5
BX-SS-C2	0.017	0.018	261.8	259.8	23.4
BX-SU-M	0.106	-	258.4	-	24.0
BX-SU-C1	0.073	0.055	269.4	240.6	135.8
BX-SU-C2	0.039	0.047	240.1	236.6	88.4

Table 4 Behaviour of composite joints

Specimen	Observed behaviour
BX-CS-M1 (monotonic negative bending)	Cracking of the concrete slab at moments of 50 kNm. Extensive concrete cracking and deformation of the end plate in the tensioned zone up to attainment of maximum moment (see Fig. 4b). Bolt failure by thread shearing at maximum moment. Failure due to loss of adherence between concrete and reinforcement.
BX-CS-M2 (monotonic positive bending)	Stiffness degradation at cracking of concrete slab, in the plane of reinforcement. Concrete crushing at the interface with the column flanges, as well as splitting of the profiled sheeting from the concrete. Failure due to cracking of the beam to end plate weld at the bottom part.
BX-CS-C1 (ECCS loading procedure)	$2e_y$ concrete cracking in tension under negative bending and concrete crushing at the column face under positive bending; $4e_y$ - degradation of concrete slab, bolt thread shearing and column flange bending; 1st $6e_y$ - bolt failure in the extended part of the connection; $6e_y$ - complete failure of the specimen.
BX-CU-M (monotonic loading)	The behaviour of the left (positive bending) and right (negative bending) connections was similar to that of the corresponding symmetrical specimens. In addition, shear deformations of the panel zone were observed. Specimen failed by cracking of the bottom beam flange weld of the right connection.
BX-CU-C1 (ECCS loading procedure)	$2e_y$ - concrete cracking; 1st $4e_y$ - maximum moment attained, extensive deformations of end plate and column flanges; $6e_y$ - bolt thread shearing, extensive cracking of the concrete slab; $8e_y$ - cracking of the Heat Affected Zone (HAZ) of the lower beam flange, propagated into the end plate by lamellar tearing (see Fig. 8b); $10e_y$ - crack spreading on the entire end plate width.
BX-CU-C2 (constant amplitude)	$6e_y$ - bolt thread shearing; 3rd $6e_y$ - cracking of the weld from beam flange; crack spreading into the beam web during successive cycles.

$f_y = 465.2$ N/mm^2, $f_u = 604.4$ N/mm^2 for $\varnothing10$ and $f_y = 425.5$ N/mm^2, $f_u = 621.7$ N/mm^2 for $\varnothing12$. The steel connectors characteristics are: $f_y = 634.9$ N/mm^2, $f_u = 641.0$ N/mm^2.

The results of tests on composite joints are summarised in Tables 4 and 5, and Figs. 4b, 7 and 8. It is to be mentioned that in the case of anti-symmetrically loaded joints, the moments on the opposite sides of the column are not equal, due to different moment capacities and connection stiffness on the two sides. Only actuator force was recorded during the tests, so that it is not possible to determine directly the moments on the two sides of the column. Therefore, a mean value of the positive and negative

Table 5 Experimental results for composite joints

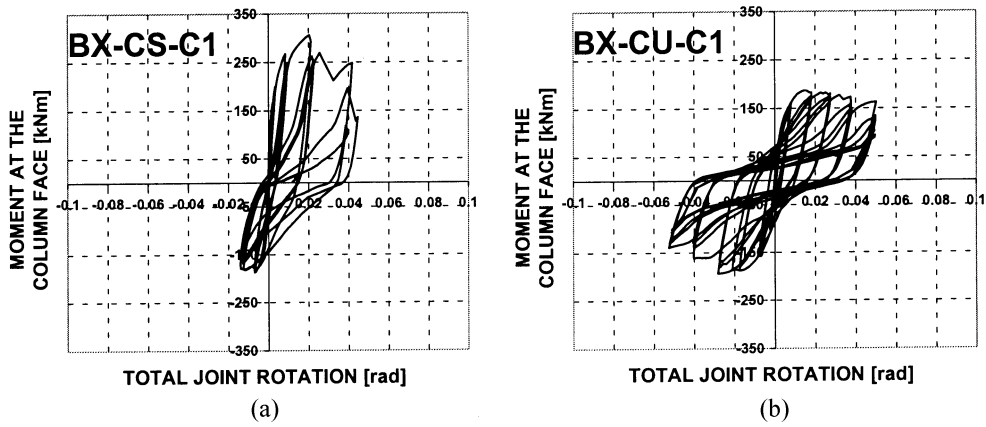| Specimen	φ_{max}^{+}, rad	φ_{max}^{-}, rad	M_{max}^{+}, kNm	M_{max}^{-}, kNm	E_{tot}, kNm rad
BX-CS-M1	-	0.087	-	244.3	16.6
BX-CS-M2	0.033	-	316.1	-	8.4
BX-CS-C1	0.045	0.014	305.5	196.9	32.0
BX-CU-M*	0.090		198.2		15.2
BX-CU-C1*	0.058		190.2		104.5
BX-CU-C2*	0.032		200.9		32.2

*Mean values

Fig. 7 Moment - rotation relationships for cyclic specimens of the BX-C series

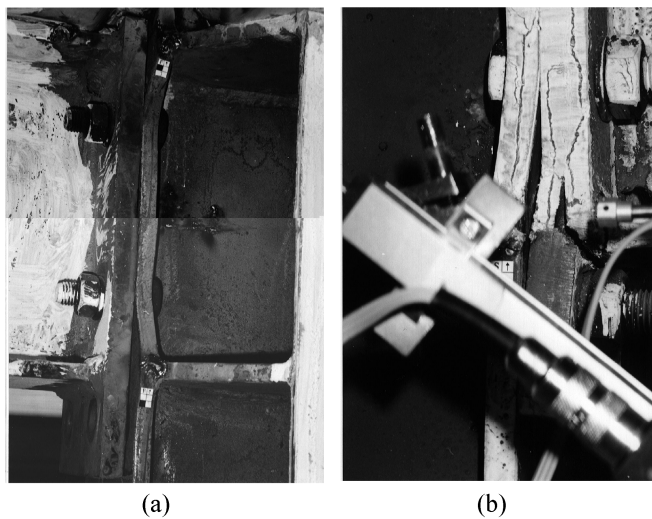Fig. 8 Failure of cyclically tested specimens form the BX-C series: BX-CS-C1 (a) and BX-CU-C1 (b)

moments was considered in the present study.

4. Comparison of test results to code results (Annex J of EC3 and EC4)

Table 6 and Table 7 presents the joint characteristics obtained from the tests and computed analytically in accordance to the Annex J of Eurocode 3 and Eurocode 4, respectively. For the

Table 6. Comparison of test to the analytical results given by Annex J of EC3 for steel joints

Specimen	Total Energy	φ_{max}^{+}	φ_{max}^{-}	M_{max}	M_{min}	$S_{j,ini}^{+}$	$S_{j,ini}^{-}$	φ_{y}^{+}	φ_{y}^{-}	M_{y}^{+}	M_{y}^{-}
	kNm rad	mrad		kNm		$\times 10^3$ kNm/rad		mrad		KNm	
Symmetrically loaded joints											
EC3-full A_s	---	---		---		55.64		2.97		165.40	
EC3red. A_s	---	---		---		55.64		2.97		165.40	
BX-SS-M	9.01	43.20		263.34		48.03		3.26		180.79	
BX-SS-C1	41.5	28.0	21.0	271.6	259.1	55.91	59.60	3.26	2.60	197.2	188.0
BX-SS-C2	23.4	17.4	18.1	261.8	259.8	71.24	63.5	2.66	2.39	194.8	206.8
Anti-symmetrically loaded joints											
EC3-full A_s	---	---		---		32.99		4.76		156.91	
EC3red. A_s	---	---		---		25.19		4.24		106.77	
BX-SU-M	24.0	105.5		258.36		51.50		2.28		137.66	
BX-SU-C1	135.8	72.5	55.3	269.4	240.6	35.07	29.08	3.77	4.44	153.1	161.2
BX-SU-C2	88.37	39.2	46.8	240.1	236.6	27.82	40.53	5.54	3.37	179.8	161.2

full A_s-full shear area approach
red A_s-reduced shear area approach, according to Annex J of EC3

Table 7 Comparison of test to the analytical results (Annex J of EC4) for composite joints

Specimen	Total Energy	φ_{max}^{+}	φ_{max}^{-}	M_{max}	M_{min}	$S_{j,ini}^{+}$	$S_{j,ini}^{-}$	φ_{y}^{+}	φ_{y}^{-}	M_{y}^{+}	M_{y}^{-}
	kNm rad	mrad		kNm		$\times 10^3$ KNm/rad		mrad		KNm	
Symmetrically loaded joints											
EC4 Mom -	---	---		---		57.11		2.34		133.80	
EC3* Mom +	---	---		---		99.68		2.30		230	
BX-CS-M1	16.60	86.7		244.25		98.47		1.27		155.51	
BX-CS-M2	8.4	32.7		316.09		105.27		2.52		231.32	
BX-CS-C1	32.0	44.8	14.1	305.5	196.9	102.5	75.05	1.60	1.73	195.2	149.9
Anti-symmetrically loaded joints											
EC4-comb.**	---	---		---		41.78		3.84		160.55	
BX-CU-M	15.2	90.1		198.24		47.19		2.34		126.23	
BX-CU-C1	104.5	60.5	53.8	187.1	193.3	36.87	37.92	3.49	3.38	142.67	137.3
BX-CU-C2	32.2	32.7	30.9	191.3	210.5	--	--	--	--	--	--

EC3* - computed according to Annex J of EC3, by translation of the centre of compression
EC4-comb.** - mean value between the positive and negative values

FULL SHEAR
AREA   shear area

SUPPLEMENTARY
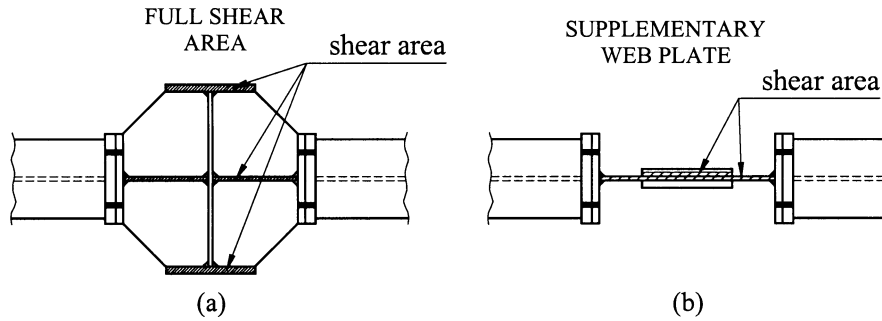WEB PLATE
shear area

(a)   (b)

Fig. 9 Full shear approach (a) and EC3 Annex J approach (b)

analytical results, the real strengths and the measured dimensions of the members have been used.
4.1. Steel joints

The Annex J of Eurocode 3 gives the possibility of computing joints having I or H cross-sections (hot rolled or built-up profiles). The main difference between the behaviour of the I shaped profiles and the X-shaped ones is the increase in the shear area of the panel zone in the latter case, due to the presence of the supplementary flanges of the column. The X-shaped cross-sectional columns can be considered in Annex J by increasing accordingly the shear area of the panel zone.

On the other hand, the Annex J specifications states that the shear area given by the panel zone can be supplemented by means of supplementary web plates, welded on one or both sides of the column web. In this way the shear area can be increased by a maximum area of $b_s t_{wc}$ (b_s - web plate width, t_{wc}- the column web thickness) from one or two supplementary web plates (Fig. 9b). In the case of X-shaped columns, due to the presence of horizontal web stiffeners, the full shear area approach should be used (Fig. 9a). The values of M_y presented in the Table 6 have been computed using both approaches, but only the full shear area approach is close to the maximum moment obtained from the tests (in the case of anti-symmetrical loading).
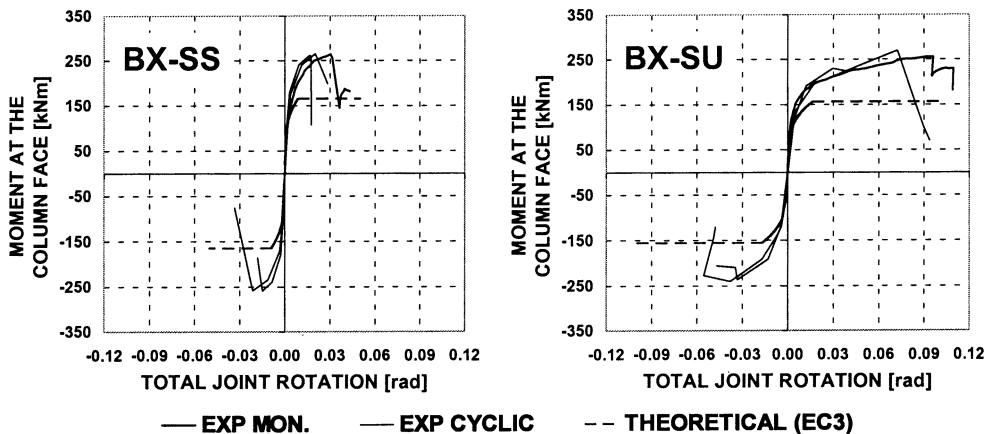
Fig. 10 Comparison of experimental results for steel joints to the EC3 Annex J predictions
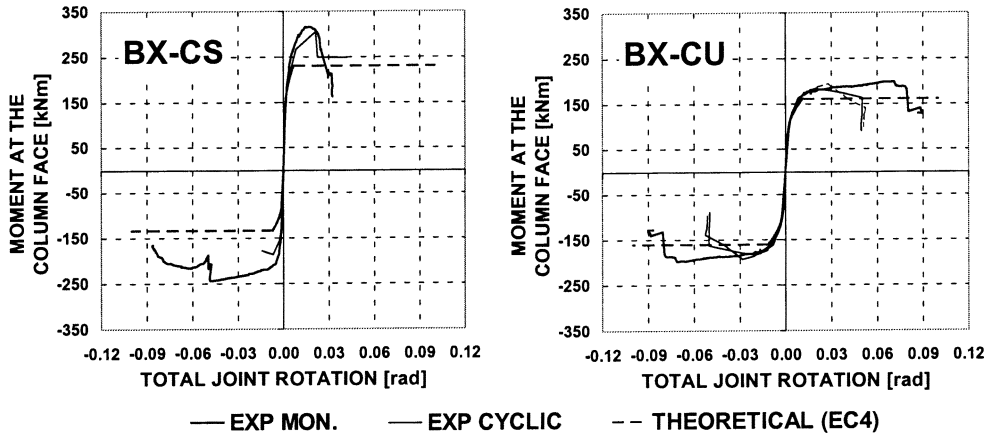
Fig. 11 Comparison of experimental results for composite joints to the EC4 Annex J predictions

The experimental curves of the monotonic tests, as well as the envelopes of the cyclic tests, are presented in Fig. 10, compared to the analytical results given by the Annex J of Eurocode 3. In the case of symmetrically loaded joints, it can be observed that the values of the experimental stiffness are close to those computed by Annex J, but the values of the computed yielding bending moment is generally 10-20% smaller than the experimental ones. For the anti-symmetrically loaded joints, only the full-shear area approach gives close agreement to the analytical results given by Annex J. The monotonic test is different from the cyclic tests in stiffness, maximum resistance and maximum rotation, as can be seen in Table 6. As usual, the maximum rotation in monotonic tests is 1.5-2 times greater than the maximum rotation attained under cyclic loading. The conventional values of yielding moment and of yielding rotation for the case of load reversal are closer to the computed values by Annex J.

4.2. Composite joints

Table 7 shows the test results, compared to the numerical ones given by Annex J. For the case of composite joints, the full shear area of the panel zone has been considered, too. Fig. 11 shows graphically the same comparison (symmetrical loading - a, anti-symmetrical loading - b). In the case of cyclic loading are shown only the envelope curves. The shear connection was computed according to EC4, part 1.6 in order to have a full-shear connection between the concrete slab and the steel beam. The studs were distributed according to the shear force pattern under gravitational loads.

The analytical computations according to Annex J of EC4 in the case of symmetrical positive bending leads to safer values in terms of resistance (15% approx.) and smaller stiffness. Due to slab degradation in cyclic tests, the resistance and stiffness values are smaller.

The Annex J of EC4 does not give the possibility of computing composite joints subjected to positive moments. For this case, the values of stiffness and moment resistance presented in Table 7 are computed according to Annex J of EC3 by a translation of the centre of compression from the upper beam flange to the middle of the concrete slab (considered without corrugated sheet). These assumptions lead to comparable values to the tests in terms of resistance and stiffness. For the case of cyclic loading, there can be observed a decrease in both resisting moment and stiffness due to rapid slab degradation.

Analytical values of moment resistance and stiffness for anti-symmetrical loading have been obtained

by the mean values for the two connections subjected to anti-symmetrical loading, taking into account the full shear area approach. This prediction remains only an attempt of computing the composite joints under anti-symmetrical loading.

5. Joint modelling

The object of a structural analysis is to have a response as close as possible to the real response of the structure. In case of moment resisting frames, the beam-to-column joints are the key-points in the dissipation of energy. Choosing a good model for joints, one can find their behaviour especially in case of load reversals, i.e. earthquake loading.

The element 14, developed for DRAIN 2DX (Prakash *et al.* 1993) at the University of Ljubljana, Slovenia, allows a sophisticate modelling of joint behaviour, starting from known characteristics obtained in experimental tests. It is a non-linear spring and permits a tri-linear non-symmetrical (positive/negative) envelope behaviour, with descending branch, as can be seen in Fig. 12. The element cyclic response is governed by special coefficients that affect the general cyclic behaviour and dissipated energy:
- α - Coefficient of descending stiffness in case of hysteretic curves
- β - Coefficient defining the moment diminution during a cycle at same amplitude
- γ - Coefficient defining the "pinching" effect (by energy method)

The model curves calibrated by the above parameters are presented in Fig. 13, for four cyclic experimental curves (steel/composite; symmetrical/anti-symmetrical loaded joints). It should be stated that the models follow closely the cyclic behaviour given by tests, and also the dissipation of energy matches globally the total energy calculates from tests.

The parameters defining the model calibrations are given in Table 8, where:
- (M_1, Φ_1), (M_2, Φ_2), (M_{max}, Φ_{max}) - pair of values that define the envelope curve M-Φ up to the maximum moment. The pairs of M-Φ values are found such that they fit best on the envelope of the experimental curve.
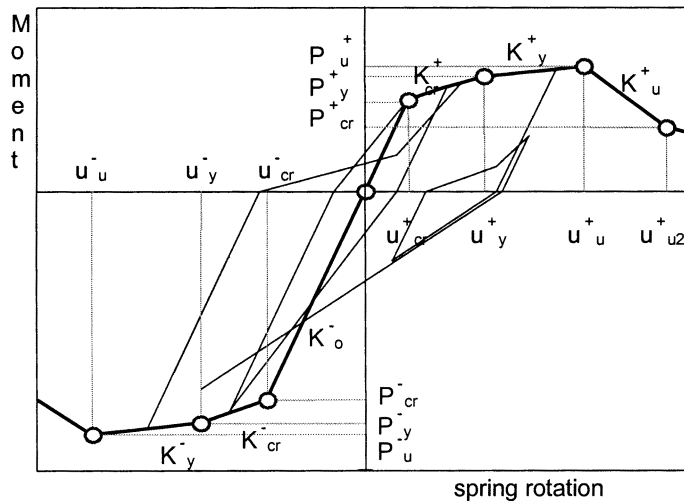

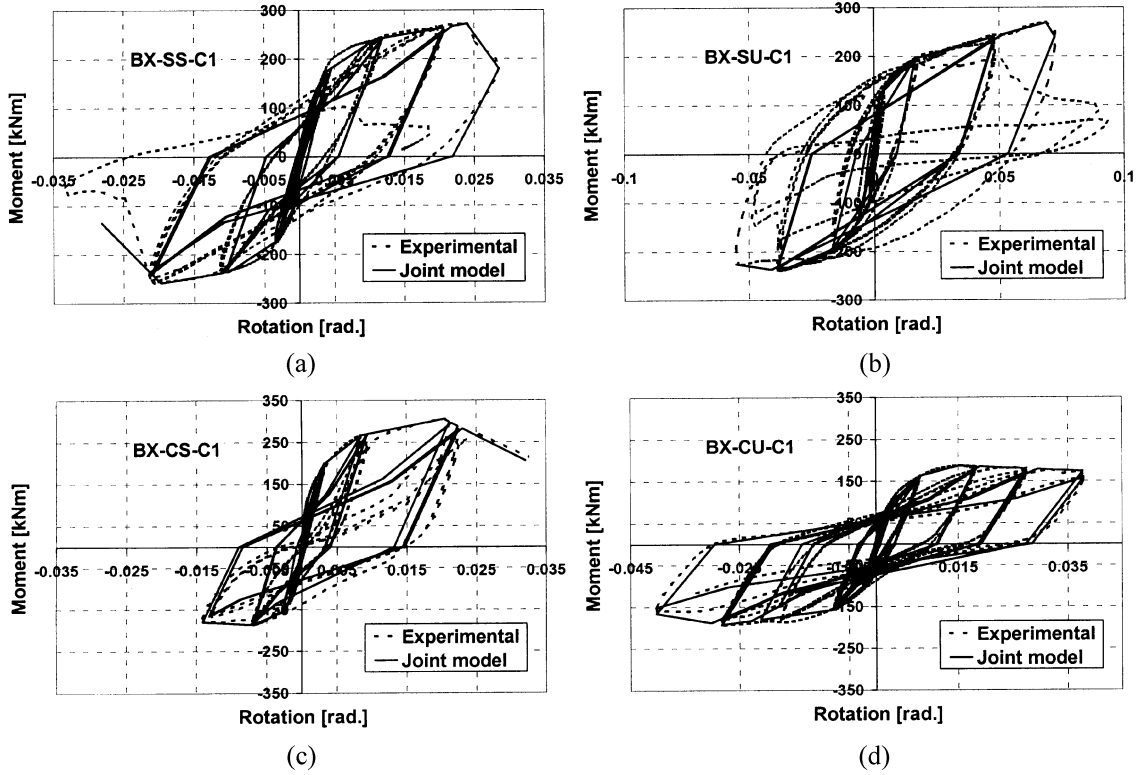Fig. 12 Joint modelling by Element 14 of DRAIN 2DX

Fig. 13 Joint modelling compared to test results

Table 8 Parameters of hysteretic curves

Specimen	Charact.	M_1	Φ_1	M_2	Φ_2	M_{max}	Φ_{max}	α	β	γ	$S_{j,desc}$
		kNm	Rad.	kNm	Rad.	kNm	Rad.	---	---	---	kNm/rad
BX-SS-C1	Pos.	98.2	0.0016	240.15	0.0109	271.57	0.024	5.99	0.007	0.847	14775
	Neg.	172.7	0.0033	235.6	0.0105	259.1	0.021	3.49	0.007	0.746	-20032
BX-SU-C1	Pos.	102.57	0.0026	195.22	0.0149	269.36	0.0375	5.67	0.005	1.0	-8171
	Neg.	81.72	0.0018	191.22	0.0164	240.59	0.0687	10	0.005	1.0	-794.6
BX-CS-C1	Pos.	117.0	0.0008	266.91	0.0085	305.52	0.0204	4.83	0.008	0.813	-5782.08
	Neg.	113.3	0.0012	155.03	0.0026	186.90	0.00689	3.27	0.003	0.880	-953.04
BX-CU-C1	Pos.	94.58	0.0024	162.42	0.0081	187.05	0.0152	4.92	0.004	0.808	-619.33
	Neg.	101.76	0.0024	181.7	0.0174	193.26	0.0282	4.63	0.005	0.818	-2223.81

• $S_{j,desc}$ the value of stiffness defining the descending branch. Usually it is very difficult to find a characteristic value of the descending branch of an experimental curve, due to its own characteristic in post-critical behaviour (rapid loss of strength), so an intermediate value is considered.

• α, β, γ - coefficients that define the hysteretic behaviour. Generally, these parameters are characteristic for each cycle, but a mean value for the entire curve is considered for each parameter, so that to have a

global energetic balance for the curve.

It can be concluded that joint models (element 14) presented herein can offer a good tool for a computer structural analysis by DRAIN 2DX code, following the experimental curves with good approximation. A detailed structural MRF analysis using joint modelling combined with realistic models of beams and columns could be found elsewhere (Ciutina *et al*. 2001).

6. Conclusions

The use of X-shaped columns makes possible a convenient design for three- and four- way connections for space moment resisting frames. Also, it brings important advantages to the joint behaviour under anti-symmetrical loading over usual I or H shaped columns. Column flanges parallel to the considered web lead to a natural stiffening of the column panel zone. This increase in the panel zone shear area reduces significantly the drop in moment capacity for anti-symmetrically loaded joints with respect to symmetrical ones, but reduces to some extent the initial stiffness. Anyway, the stiffened panel zone participates to the plastic mechanism, assuring a significantly increased ductility of anti-symmetrically loaded joints.

Cyclic loading introduces differences between the type of failure of both bare steel and composite joints. While for monotonic tests the failure was mainly by bolt failure and column flange/end plate deformations, in the case of cyclic tests it was by brittle failure of the fillet welds. Therefore, particular care is needed in design and manufacture of the welds in zones with load reversals. Full-penetration welds could be more reliable. However, weld quality is of paramount importance.

The cyclic loading reduces the ductility of bare steel and composite joints. Roughly, the maximum rotation of cyclically loaded joints is 50% of the monotonically loaded ones for bare steel joints and anti-symmetrically loaded composite joints, and 33% for symmetrically loaded composite joints. However, in the case of anti-symmetrically loaded joints (which is the case under seismic loading), the plastic rotation capacity is greater than the generally accepted requirement of 0.03 rad. for special MRFs (AISC 1997). This is valid both bare steel and composite joints considered in this study. The maximum bending moment M_{max} is affected by the cyclic loading in the case of composite connections only. A 10% reduction of the maximum bending moment attained under monotonic loading could be considered as a safe estimation of the maximum bending moment under seismic loading.

Composite action of the concrete slab on the steel beam has a positive effect on the ductile behaviour of the symmetrically loaded joints under negative moments. Under positive moments, the centre of compression is shifted into the concrete slab, leading to a higher lever arm for the extreme bolt rows, and higher stiffness and moment capacity of the joint. Consequently, in the case of composite joints under positive moments, the lower steel part of the joint should be proportioned accordingly, in order to resist the increased demand due to composite action.

In the case of composite joints with partially extended end plate (at the bottom part only), the steel reinforcement in the slab is not able to compensate for the missing bolt row in the extended end plate, even if a relatively high reinforcement ratio is used (1.8% for the joint zone). A pinching behaviour could be observed for the anti-symmetrically loaded specimens, after cracking of the concrete slab. A higher strength concrete is believed to postpone this phenomena, and to result in more stable behaviour. Due to rapid degradation of the concrete slab in the case of anti-symmetrically loaded composite joints and pinching behaviour, the dissipated energy per cycle is relatively low.

A total shear connection between the concrete slab and the beam as defined by EC 4 (ENV 1994-1-1 1992) leads to an adequate performance of the connectors in the joint zone. There have been no

recorded failures of the connectors in tests performed.

Analytical model of Annex J - EC3 for steel joints and EC4 for composite joints respectively - provides a reliable prediction for behaviour of I beam to X-shaped columns with extended end plate connections, but an appropriate modelling of the panel zone should be used. When transverse stiffeners are used, the effective shear area of the X-shaped column panel zone should be considered as the sum of the shear areas of the column web and the two flanges parallel to the considered web (Dubina *et al*. 2000b).

The experimental results of composite joints and the EC 4 Annex J predictions shows a good agreement, the code offering a good basis for design of composite joints under negative bending. For design of composite joints under positive bending, Annex J provisions could be used, but taking the centre of compression shifted into the concrete slab. In case of anti-symmetrical loading an adequate modelling should be found.

New modern seismic codes (AISC 1997), based on experimental proofs of structural beam-to-column joints, classify the joints by different levels of ductility and resistance but they do not offer the verification tool for structural analysis. The joint modelling that is permitted by element 14 of DRAIN 2DX, accompanied by similar models for structural members can offer a solution to this issue. These models give results close to reality, for an accurate structural analysis, especially in the post-elastic domain where the quantity and location of energy dissipation becomes important. In the case of a design based on performance criteria (Bertero 1997), such modelling could be considered as the controlling tool for the required criteria.

References

AISC 97 (1997), *Seismic Provisions for Structural Steel Buildings.* American Institute of Steel Construction, Inc. Chicago, Illinois, USA.

Bertero V. (1997), "General report on codification, design and applications", - *STESSA 97 Behaviour of Steel Structures in Seismic Areas, Proceedings of the Second International Conference* 3-8 Aug. 1997, Kyoto, Japan.

Ciutina, A, Stratan A. and Dubina D. (2001), "Răspunsul Seismic al Cadrelor Metalice Multietajate în funcþie de modelele *M-Φ* utilizate pentru îmbina ˘ ri şi elemente structurale", *Proc. the Second Nat. Conf. on Earthquake Engineering - UAICR*, Bucureşi, 8-9 November, 2001, Vol 2, 3.113-3.123.

Dubina, D., Grecea, D., Ciutina, A. and Stratan, A. (2000), "Influence of connection typology and loading asymmetry", Chapter 3.2 in: *Moment Resistant Connections of Steel Building Frames in Seismic Areas -*, (Mazzolani F.M. ed.) E&FN SPON (London).

Dubina, D., Stratan, A. and Ciutina, A. (2000), "Cyclic tests on bolted steel double-sided beam-to-column joints", NATO Advanced Research Workshop. *The Paramount Role of Joints into the Reliable Response of Structures.* From the Rigid and Pinned Joints to the Notion of Semi-rigidity. Ouranoupolis, Greece, 21-23 May 2000.

Dubina, D., Ciutina, A. and Stratan, A. (2001), "Cyclic tests of double-sided beam-to-column joints", *J. Struct. Eng.*, **127**(2), 129-136.

ECCS (1985), *Recommended Testing Procedures for Assessing the Behaviour of Structural Elements under Cyclic Loads*, European Convention for Constructional Steelwork, Technical Committee 1, TWG 1.3 Seismic Design, No. 45.

ENV 1993-1-1 (1997), EUROCODE 3: *Part 1.1. Revised Annex J: Joints in Building Frames. Approved Draft: January 1997*; CEN, European Committee for Standardisation.

ENV 1994-1-1 (1992), EUROCODE 4: *Part 1.1. General rules and rules for buildings*; CEN, European Committee for Standardisation.

Moisa, T., Pascu, R. and Romanu, R. (2000), "Study on causes of weld fractures in extended end-plate connections under cyclic loads", *Report No. 409/1999.* Institute of Welding and Testing of Materials (ISIM) - 2000.

Prakash V., Powell G.H. and Campbell S. (1993), *DRAIN 2DX Base Program Description and User Guide,* Berkeley University of California, 1993.

CK